Nonlinear Atom Interferometry

David Wakeham,[1] Julian Werther,[1,2] and Philipp Stephan[1,2]

[1] *Department of Physics and Astronomy, University of British Columbia 6224 Agricultural Road, Vancouver, British Columbia, Canada, V6T 1Z1*
[2] *Fukultät für Physik und Astronomie, Julius-Maximilians-Universität Würzburg Am Hubland, 97074 Würzburg, Germany*

Interferometry exploits interference effects to make measurements. Although interferometers are traditionally optical, due to wave-particle duality they can just as well use matter waves, as in the atom-based Ramsey-Bordé interferometer. A Bose-Einstein condensate of two-level bosons has an effective nonlinear interaction, which can be used to create a nonlinear Ramsey-Bordé interferometer. Recently, such nonlinear BEC interferometers have surpassed classical constraints on precision of measurement.

I. INTRODUCTION

Interferometry has been an important tool for precision measurements for a long time. Classically the effects of interference have been studied and utilized on electromagnetic waves. With the emergence of quantum mechanics and de Broglie's prediction of the wave-like nature of matter, interest in matter-based interferometry arose [1]. Due to their ease of use, the first kind of particles studied in this manner were electrons. As techniques and precision progressed, the race for ever shorter de Broglie wavelengths began and the next step was the neutron interferometer [2]. The latest milestone is the overcoming of the classical limit (discussed below), leveraging nonlinear atom interferometry [3].

This article will focus on an experimental realization of nonlinear interferometry in the form of the *nonlinear atom interferometry*, reviewing the theoretical background and connection to metrology. Example applications for nonlinear interferometers are provided, and we finish with an outlook on the field.

II. ATOM INTERFEROMETRY

A. Basic setup

In quantum mechanics, particles also exhibit wave-like properties. De Broglie found that by virtue of their momentum, particles have a wavelength of

$$\lambda_{\mathrm{dB}} = \frac{h}{mv}\,, \tag{1}$$

where m denotes the particles mass, v its velocity and h is Planck's constant. Therefore atom waves show interference and can be used for interferometry in principle.

Before progressing to atom interferometry, a few principles from optical intereferometry will be stated. This paragraph follows mainly [4].

a. Preparation of the initial beam. If the initial states are localized in space, then the momentum uncertainty will spread out [5]. Since interferometry actually occurs in momentum space, therefore, it is better to keep momentum as a good quantum number. So the preparation must be in the momentum space. Furthermore, to get coherent atom waves with free atoms, we have to reduce the momentum and its uncertainty. One way of doing this is cooling the system down to low temperatures.

b. Manipulation. In optical interferometry, half-silvered mirrors are often used as beam splitters, but this does not work for atomic waves because the atoms would be absorbed or scattered in the solid matter. Resonant stationary laser waves or light pulses can diffract atom waves and can be used as a beam splitter instead.

In the case of the stationary laser wave, the atom wave (orthogonal to the laser wave) would be split into excited states with either $\mathbf{p}+\hbar\mathbf{k}_{\mathrm{ph}}$ or $\mathbf{p}-\hbar\mathbf{k}_{\mathrm{ph}}$, where $\mathbf{k}_{\mathrm{ph}}$ denotes a laser photon's momentum vector [6]. This is a direct result of the momentum conservation, assuming an elastic process with the resonant condition $\hbar\omega_{\mathrm{ph}} = E_{\mathrm{ex}} - E_{\mathrm{gs}}$, where ω_{ph} is the angular frequency of the photon, E_{ex} the energy of the excited state, and E_{gs} the ground state [6]. When the photon energy is not equal to this energy difference, there is an additional phase shift. Furthermore, the atom wave does not experience a recoil at the nodes of the standing wave. The Bragg condition $\sin\theta = \lambda_{\mathrm{dB}}/(2\lambda_{\mathrm{ph}})$ for the first maximum can only be satisfied when $\lambda_{\mathrm{dB}} \approx \lambda_{\mathrm{ph}}$, but this is usually the case for ultracold atoms or short optical wavelength [6].

In the second case where laser pulses are used as beam splitters only one momentum $\mathbf{p} + \hbar\mathbf{k}_{\mathrm{ph}}$ can contribute to the splitting. This results in the momentum split state [7]

$$a_{\mathrm{gs}}\,|\mathrm{gs}\rangle \otimes |\mathbf{p}\rangle + a_{\mathrm{ex}}\,|\mathrm{ex}\rangle \otimes |\mathbf{p} + \hbar\mathbf{k}_{\mathrm{p}}\rangle\ . \tag{2}$$

The coefficients a_{gs} and a_{ex} of the ground state and the excited state depend mainly on the laser power and the beam profile. An ideal beam splitter can be achieved when the coefficients are equal $|a_{\mathrm{gs}}| = |a_{\mathrm{ex}}|$. This is satisfied when the laser pulse is of duration $T = \pi/(2\omega_{\mathrm{ph}})$ [7]. Those $\pi/2$-pulsed optical beam splitters are also used in the Ramsey-Bordé atom interferometer. A pulsed laser beam also provides a way of performing time-domain operations in interferometry [6].

c. Detection. After recombination of the two split matter waves with the use of diffraction on optical light,

the interference fringes and the phase difference ϕ can be observed as an imbalance in atomic populations at two output ports. The imbalance oscillates sinusoidally depending on ϕ and is called a *Ramsey fringe* [4].

B. Ramsey-Bordé atom interferometer

The starting point of the development of the Ramsey-Bordé atom interferometer is the *separation of oscillating field method*, devised by Ramsey in 1950 [8]. With this technique, Ramsey explained how the diffraction of matter waves on optical light could be used for beam splitting.

C. Bordé improved Ramsey's idea by using four pulsed laser beams (see figure 1) [9]. The incoming coherent matter wave in the ground state $|a, 0\rangle$ from the left side will first be split by a $\pi/2$ laser pulse. The second and the third laser beams are π-pulsed and act on the states like a mirror, which means that the states are just flipped. Finally, the last laser beam is again $\pi/2$-pulsed and recombines the two states. This geometrical configuration is comparable to the optical Mach-Zehnder interferometer [10] and it is common to illustrate the experimental setup this way.

In fact, two $\pi/2$-pulses would be enough for doing atom interferometry, but Bordé's four interaction zone method offers the advantage that the interference maxima are free of Doppler-shifts to linear order, so those interference fringes do not wash out [11]. A Ramsey-Bordé atom interferometer as depicted in figure 1 only works if the lifetime of the excited state $|b, m_b\rangle$ is longer than the transition time. Otherwise, the coherence of the matter wave is destroyed [4].

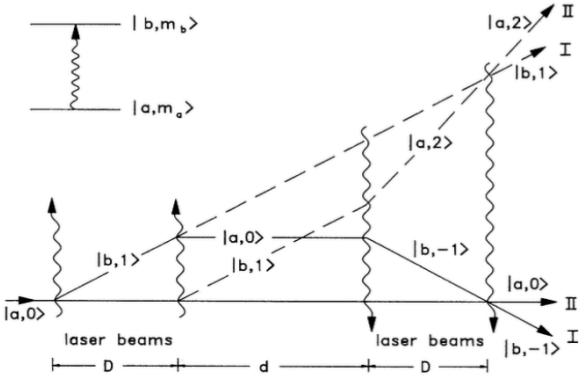

Figure 1: The principal configuration of a Ramsey-Bordé atom interferometer [12]. This is usually characterized by four laser beams which influence the matter wave. The first and the last one act like 50/50 beam splitter, because those are $\pi/2$-pulsed, while the two other laser beams are π-pulsed and act like mirrors. Here $|a, m_a\rangle$ denotes the ground state and $|b, m_b\rangle$ the excited state, where m represents the number of photon recoils. The solid lines show the path of the high frequency component of the interferometer, whereas the dashed lines show the low frequency path.

III. BEATING THE CLASSICAL LIMIT

A. Quantum metrology

More broadly, interferometry is one strategy for performing measurement: preparation of a probe, interaction with the system to be measured, and probe readout [13]. The *sensitivty scaling* of a measurement scheme relates the resources used in probe design and the size of the measurement error. An atom interferometer measures a phase difference ϕ, and the relevant probe resource is the number of particles N in the coherent matter wave [3, 14]. The *classical limit* (also called the *standard quantum limit*) is the scaling $\Delta\phi \propto 1/\sqrt{N}$. This arises via the central limit theorem when components of the matter wave interact independently, and is the optimal scaling for linear interferometry.

Improving on the classical limit requires entanglement, many-body interactions, or both [14], but the fundamental constraint is Heisenberg's uncertainity principle, leading to the *Heisenberg limit* $\Delta\phi \propto 1/N$ [13]. Experimentally, the classical limit can be surpassed using a nonlinear Ramsey-Bordé atom interferometer made from ultra-cold gas [3], which we will now discuss.

B. Bose-Einstein condensates

a. Gross-Pitaevskii equation. Consider a gas of weakly interacting bosons in a confining potential. At low temperatures, a sizeable fraction of particles condense into the ground state, forming a *Bose-Einstein condensate* (BEC) [15]. A BEC can be described by a mean-field *condensate wavefunction* $\psi(\mathbf{r}) \equiv \sqrt{n(\mathbf{r})}\, e^{i\theta(\mathbf{r})}$, where $n(\mathbf{r})$ is the average density and $\theta(\mathbf{r})$ the phase. The Schrödinger equation governing $\psi(\mathbf{r})$ (to leading order in N) is the *Gross-Pitaevskii equation* (GPE):

$$\left(-\frac{\hbar^2}{2m}\nabla^2 + V(\mathbf{r}) + gn(\mathbf{r})\right)\psi(\mathbf{r}) = \mu\psi(\mathbf{r}) \qquad (3)$$

where $V(\mathbf{r})$ is the *trapping potential*, μ is the chemical potential, and g is a coupling related to the *s-wave scattering length* a by $g \equiv 4\pi\hbar^2 a/m$.

b. Josephson approximation. Suppose our BEC consists of N two-level bosons, with hyperfine states $|1\rangle$ and $|2\rangle$. In the *Josephson approximation*, the BEC wavefunction factorises into the condensate wavefunction $\Psi(\mathbf{r})$ and hyperfine occupation modes, with elastic (number-conserving) transitions between the latter [16]. The effec-

tive Hamiltonian

$$\hat{H} = NE_0 + \frac{1}{2}\eta \sum_{\alpha,\beta=1}^{2} g_{\alpha\beta} a_\beta^\dagger a_\alpha^\dagger a_\alpha a_\beta \,, \tag{4}$$

consists of the sum of (mean-field) single particle energies NE_0, and two-body scattering, where $a_i^\dagger(a_i)$ creates (annihilates) a state in mode $|i\rangle$, $g_{\alpha\beta}$ is the coupling for the transition process, and η is a normalization constant. Rewriting equation (4) in terms of the (Schwinger) angular momentum operator [17]

$$\hat{J}_z = \frac{1}{2}(a_1^\dagger a_1 - a_2^\dagger a_2) \,, \tag{5}$$

and ignoring constants, we obtain

$$\hat{H} = \gamma_1 \eta N \hat{J}_z + \gamma_2 \eta \hat{J}_z^2 \,, \tag{6}$$

where $\gamma_1 \equiv (g_{11} - g_{22})/2$ and $\gamma_2 \equiv (g_{11} + g_{22})/2 - g_{12}$. We can also apply microwave and radio-frequency pulses in some direction $\hat{\mathbf{n}}$ in the x-y plane to the system to drive *Rabi oscillations* with frequency Ω, effectively coupling the hyperfine modes (at the single particle level). This leads to a final Hamiltonian of the form

$$\frac{1}{\hbar}\hat{H} = \Delta\omega \hat{J}_z + \chi \hat{J}_z^2 + \Omega\, \mathbf{J} \cdot \hat{\mathbf{n}} \,, \tag{7}$$

where $\Delta\omega \equiv \gamma_1 \eta N/\hbar$ is a *detuning resonance* affecting the relative phase acquired during free evolution, and $\chi \equiv \gamma_2 \eta$ gives the size of the effective *nonlinear* interaction. Note that g_{12}, and hence χ, can be magnetically tuned. This quadratic interaction allows us to perform nonlinear interferometry; it is analogous to the the KERR nonlinearity in optics, where a material has a refractive index proportional to the intensity of light, $n \propto |E|^2$ [17].

c. Bloch sphere. The *Bloch sphere* is a convenient way of representing a two-level system $|1\rangle$, $|2\rangle$ such as our hyperfine states, pictured in figure 2(a). Any pure state can be written as a superposition

$$|\theta, \phi\rangle \equiv \sin(\theta/2)\,|2\rangle + \cos(\theta/2)\,\mathrm{e}^{\mathrm{i}\phi}\,|1\rangle \,, \tag{8}$$

such that $|\theta, \phi\rangle$ is an eigenvector of $J_n \equiv \hat{\mathbf{n}}|\theta, \phi\rangle \cdot \mathbf{J}$. This can be generalized to coherent state of N two-level atoms [17]

$$|\theta, \phi\rangle \equiv \frac{1}{\sqrt{N!}} \left(\sin(\theta/2)\,\hat{a}_2^\dagger + \cos(\theta/2)\,\mathrm{e}^{\mathrm{i}\phi}\,\hat{a}_1^\dagger\right)^N |0\rangle \,. \tag{9}$$

We can implement nonlinear interferometry by running the Josephson Hamiltonian equation (7) on a coherent state, and controlling Ω and χ. In particular, the nonlinear interaction generates *squeezed states* [18], discussed below.

C. Nonlinear interferometry and the precision limit

In 2010 GROSS *et al.* surpassed the classical precision limit with a Ramsey-Bordé atom interferometer using a Bose-Einstein condensate of rubidium ^{87}Rb and a nonlinear beam splitter [3, 17]; similar results were obtained in [16]. The hyperfine structure of the $5^2S_{1/2}$ state in ^{87}Rb with the Zeeman splitting is a suitable two-level system.

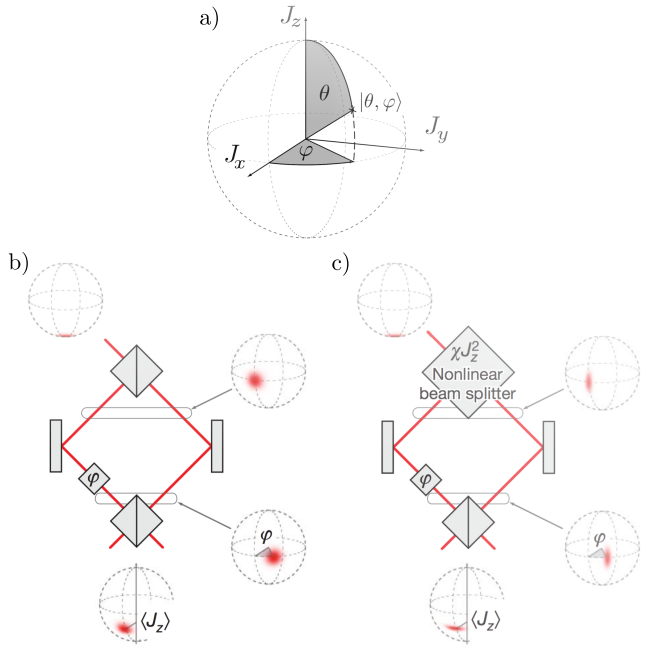

Figure 2: Plane a) illustrates the Bloch sphere of a spin 1/2 particle with the spin axes $\hat{J}_x$, $\hat{J}_y$, and $\hat{J}_z$. The linear and nonlinear Ramsey–Bordé atom interferometers are presented in b) and c), where those configurations are visualized in style of the optical Match-Zehnder interferometer. Additionaly the interaction of the different components to the state on the Bloch sphere is illustrated. Figure adapted from [17].

Due to the uncertainty principle (and the angular momentum commutation relations), it is impossible to measure the polar angle θ and azimuthal angle ϕ to arbitrary precision. For a coherent and isotropic spin state the angular uncertainty is given by $\Delta\phi = \Delta\theta = 1/\sqrt{N}$ [17]. The angular uncertainty for the linear (figure 2(b)) and nonlinear (figure 2(c)) Ramsey-Bordé interferometer after the different steps is visualized on the Bloch sphere. The nonlinear beam splitter acts like a noise tomograph and is responsible for creating *spin-squeezed states*.

Unlike coherent states, spin-squeezed states are entangled, with anisotropic fluctuations of the spin vector $\Delta J_\perp$ perpendicular to the total mean spin J. This is surprising, since each *single* spin fluctuation is still isotropic. In order to comply with the Heisenberg uncertainty relation, reducing the variance in one perpendicular direction increases the variance in the other. The *squeezing parameter*, which quantifies the anisotropy, is defined as [17]

$$\xi^2 \equiv N \frac{\Delta \hat{J}_\perp^2}{\langle \hat{\mathbf{J}} \rangle^2} = N \frac{\Delta \hat{J}_z^2}{\langle \hat{J}_x \rangle^2}. \tag{10}$$

A state is squeezed if $\xi^2 < 1$.

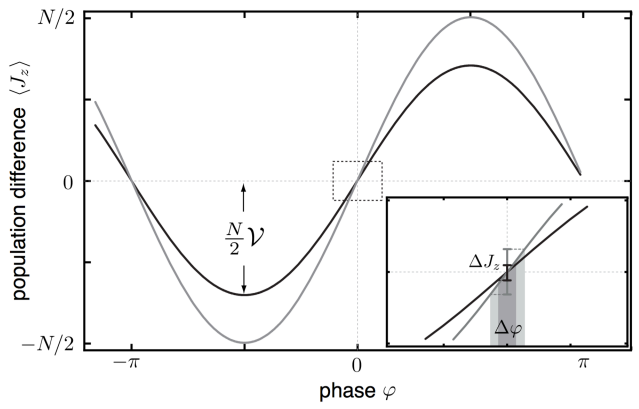

Figure 3: The population difference $\langle \hat{J}_z \rangle$ of the Ramsey fringes vs the phase for linear and nonlinear Ramsey-Bordé atom interferometer are shown here. The maximum value of the population differance is given by: $\langle \hat{J}_z \rangle = N\mathcal{V}/2$, where N is the number of atoms and $\mathcal{V}$ the visibility [3].

The interferometric procedure of figure 2(b) is as follows. A coherent BEC state is produced by coupling modes via pulses with Rabi frequency Ω. The nonlinear interaction $\chi \hat{J}_z^2$ is briefly "switched on" by magnetic tuning, and acts as a beamsplitter, splitting the coherent states into spin-squeezed states [18]. The squeezed beams separately evolve according to equation (7), with $\chi \approx 0$, acquiring a relative phase ϕ which translates into an observable mean population difference $\langle \hat{J}_z \rangle$ when the beams are recombined using the standard linear $\pi/2$-pulse [3]. The squeezing leads to reduced noise in $\langle \hat{J}_z \rangle$, which ultimately lets us beat the classical limit. Put a different way, the nonlinearity entangles the beams, and that entanglement leads to super-classical precision.

Figure 3 illustrates the population difference $\langle \hat{J}_z \rangle$ versus the phase ϕ for an *ideal* linear interferometer (grey) and the experimentally realized nonlinear atom interferometer (black). The variance of the angle

$$\Delta\phi^{-1} = \left(\frac{\Delta \hat{J}_z}{\partial_\phi \langle \hat{J}_z \rangle} \right)^{-1} \tag{11}$$

depends on the variance of spin $\Delta \hat{J}_z$ and the slope of the Ramsey fringe $\partial_\phi \langle \hat{J}_z \rangle$ [17]. The sensitivity or variance of the angle is maximal where the population of spin is zero. In other words, the slope must be maximal to achieve optimal sensitivity for the Ramsey-Bordé interferometer. From figure 3, we can see that the nonlinear interferometer is more sensitive than the ideal linear interferometer, with Gross *et al.* reporting a 31 % improvement in phase precision [17]. Although the precise scaling would require more experiments, the comparison to the ideal linear interferometer is sufficient to show improvement on the classical limit.

IV. APPLICATIONS

Since one of the main characteristics of nonlinear interferometry is its enhanced precision compared to the classical case, it is very well suited for precision measurements.

A big area of application is the measurement of inertial effects. These are often very small by nature and therefore a high sensitivity is desirable. As matter-based interferometers are very sensitive to inertial effects, they are well suited for this kind of measurement [19]. Various groups have used nonlinear interferometers to measure the gravitational acceleration g on the earth's surface,[20, 21] as well as Newton's gravitational constant G [22, 23].

The interferometers of Ramsey type described in the text above are especially well suited for this purpose [17]. Kasevich *et al.* describe a method to measure gravitational acceleration to a precision of $10^{-10}\, g$ [20].

Measurements of the earth's rotation and the corresponding Coriolis force have also been performed [19, 24].

Another utilization of the Ramsey scheme is the high precision measurement of atomic oscillations. These are then in turn used to define a time standard and build highly accurate clocks. In 1999 Santarelli *et al.* were able to improve the precision of their clock by a factor of five utilizing Ramsey oscillations [25].

V. SUMMARY

In this paper we provided a brief overview of nonlinear atomic interferometry.

In section II, a brief review of classical interferometry is provided and compared to matter based methods. Then a experimental setup of a Ramsey-Bordé interferometer is described as an illustration of an atom interferometer. On this example the ability of a *nonlinear* interferometer to surpass the classical limit is demonstrated. In this case the precision was increased by about 31 % [3].

Section III first introduces the general principles of measurements before progressing to a brief overview of Bose-Einstein condensates. After that, the theory behind nonlinear interferometry and why it can surpass the classical limit is discussed.

[1] L. de Broglie, The London, Edinburgh, and Dublin Philosophical Magazine and Journal of Science **47**, 446 (1924), https://doi.org/10.1080/14786442408634378, URL https://doi.org/10.1080/14786442408634378.

[2] C. S. Adams, Contemporary Physics **35**, 1 (1994).

[3] C. Gross, T. Zibold, E. Nicklas, J. Estève, and M. K. Oberthaler, Nature **464**, 1165 (2010), ISSN 0028-0836.

[4] A. Cronin, J. Schmiedmayer, and D. Pritchard (2007).

[5] L. Mandel and E. Wolf, *Optical coherence and quantum optics* (Cambridge university press, 1995).

[6] C. J. Bordé, Atom Interferometry p. 257 (1997).

[7] J. Baudon, R. Mathevet, and J. Robert, Journal of Physics B: Atomic, Molecular and Optical Physics **32**, R173 (1999).

[8] N. F. Ramsey, Phys. Rev. **78**, 695 (1950).

[9] C. Bordé, Physics Letters A **140**, 10 (1989), ISSN 0375-9601.

[10] P. Hariharan, *Basics of interferometry* (Academic Press, 2010).

[11] T. Nazarova, Ph.D. thesis, University of Hannover (2007).

[12] F. Riehle, T. Kisters, A. Witte, J. Helmcke, and C. J. Bordé, Physical review letters **67**, 177 (1991).

[13] V. Giovannetti, S. Lloyd, and L. Maccone, Nature photonics **5**, 222 (2011).

[14] S. Boixo, A. Datta, S. T. Flammia, A. Shaji, E. Bagan, and C. M. Caves, Phys. Rev. A **77**, 012317 (2008).

[15] S. Haroche and J.-M. Raimond, *Exploring the quantum: atoms, cavities, and photons* (Oxford university press, 2006).

[16] A. B. Tacla, S. Boixo, A. Datta, A. Shaji, and C. M. Caves, Phys. Rev. A **82**, 053636 (2010).

[17] C. Gross, Ph.D. thesis, University of Heidelberg (2010).

[18] M. Kitagawa and M. Ueda, Phys. Rev. A **47**, 5138 (1993).

[19] A. Miffre, M. Jacquey, M. Büchner, G. Trénec, and J. Vigué (2006), arXiv:quant-ph/0605055.

[20] M. Kasevich and S. Chu, Applied Physics B: Lasers and Optics **54**, 321 (1992).

[21] A. Peters, K. Y. Chung, and S. Chu, Metrologia **38**, 25 (2001).

[22] A. Bertoldi, G. Lamporesi, L. Cacciapuoti, M. de Angelis, M. Fattori, T. Petelski, A. Peters, M. Prevedelli, J. Stuhler, and G. M. Tino, The European Physical Journal D - Atomic, Molecular, Optical and Plasma Physics **40**, 271 (2006), ISSN 1434-6079, URL https://doi.org/10.1140/epjd/e2006-00212-2.

[23] M. Fattori, G. Lamporesi, T. Petelski, J. Stuhler, and G. Tino, Physics Letters A **318**, 184 (2003).

[24] T. Gustavson, P. Bouyer, and M. Kasevich, Physical Review Letters **78**, 2046 (1997).

[25] G. Santarelli, P. Laurent, P. Lemonde, A. Clairon, A. G. Mann, S. Chang, A. N. Luiten, and C. Salomon, Physical Review Letters **82**, 4619 (1999).